Atmospheric Blocking Drives Recent Albedo Change Across the Western Greenland Ice Sheet Percolation Zone

Lewis, Gabriel[1,2]; Osterberg, Erich[1]; Hawley, Robert[1]; Marshall, Hans Peter[3]; Meehan, Tate[3]; Graeter, Karina[1]; McCarthy, Forrest[1]; Overly, Thomas[1,4]; Thundercloud, Zayta[1]; Ferris, David[1]; Koffman, Bess[5]; Dibb, Jack[6]

[1]Department of Earth Sciences, Dartmouth College, Hanover, NH, USA

[2]Department: Natural Resources & Environmental Science, University of Nevada Reno, Reno, NV, USA

[3]Geosciences Department, Boise State University, Boise, ID, USA

[4]NASA Cryospheric Sciences Laboratory, NASA Goddard Space Flight Center, Greenbelt, MD, USA

[5]Geology Department, Colby College, Waterville, ME, USA

[6]Institute for the Study of Earth, Oceans, and Space, University of New Hampshire, Durham, NH, USA

Corresponding author: Gabriel Lewis (Gabriel.M.Lewis.GR@Dartmouth.edu)

Key Points:

- Larger surface snow grain size significantly decreases albedo across the western Greenland Ice Sheet percolation zone.
- Black carbon and dust concentrations are too low to significantly affect albedo in the percolation zone.
- Strong atmospheric blocking decreases albedo by enlarging grain sizes via fewer storms (less fresh snow) and fewer optically thick clouds.

Abstract

Greenland Ice Sheet (GrIS) albedo has decreased over recent decades, contributing to enhanced surface melt and mass loss. However, it remains unclear whether GrIS darkening is due to snow grain size increases, higher concentrations of light-absorbing impurities (LAIs), or a combination. Here, we assess albedo controls in the western GrIS percolation zone using in situ albedo, LAI, and grain size measurements. We find a significant correlation between albedo and snow grain size ($p < 0.01$), but not with LAIs. Modeling corroborates that LAI concentrations are too low to significantly reduce albedo, but larger grain sizes could reduce albedo by at least ~3%. Strong atmospheric blocking increases grain sizes and reduces albedo through increased surface temperature, fewer storms, and higher incoming shortwave radiation. These findings clarify the mechanisms by which anomalously strong blocking contributed to recent GrIS albedo decline and mass loss, highlighting the importance of improving projections of future blocking.

Plain Language Summary

Remote sensing and computer models have shown that the reflectivity (or albedo) of the Greenland Ice Sheet has decreased in recent decades, causing increased melt and sea level rise. It is unknown whether this albedo decline is due to increased impurities in the snow, larger snow grain sizes, or both. Field measurements show that the amount of impurities is too small to affect albedo in our field area. However, larger snow grain sizes could lower albedo enough to cause the observed trend. We demonstrate how a recent increase in the frequency of atmospheric high pressure systems over Greenland increases grain sizes via several mechanisms and contributes to Greenland's observed albedo decline and faster melt.

1. Introduction

Albedo is a critical component of Greenland surface mass balance (SMB) because of its role in temperature feedbacks that enhance snowmelt, runoff, and global sea level rise (Alexander et al., 2014). Even a small decrease in albedo is important to SMB; a decrease of fresh snow albedo of 0.01 over a three-year period would result in a surface mass loss > 25 Gt a^{-1} (Dumont et al., 2014). Satellite measurements from the MODerate resolution Imaging Spectroradiometer (MODIS) indicate that Greenland albedo has been declining since 2000 (Hall et al., 2018; Wright et al., 2014; Zwally et al., 2005, 2011; see Figure 1a), even after correcting for MODIS sensor

degradation (Casey et al., 2017; Polashenski et al., 2015). However, it is unclear whether the GrIS darkening is due to snow grain size increases from warmer air temperatures (Box et al., 2012), higher concentrations of light-absorbing impurities (LAI) like soot and dust (Dumont et al., 2014), or some combination of these causes.

The GrIS surface has warmed by at least 2.7 °C since 1982 (van den Broeke et al., 2009; De La Peña et al., 2015; McGrath et al., 2013), producing the highest rates of surface melt and runoff in at least 450 years and most likely ~7000 years (Graeter et al., 2018; Trusel et al., 2018). A melting snowpack causes snow optical grain sizes (OGSs) to increase, which lowers the broadband albedo (Warren and Wiscombe, 1980). In addition, black carbon (BC) soot, a by-product of biomass and fossil fuel combustion, absorbs solar radiation more efficiently than other LAIs, especially in the visible wavelengths (Flanner et al., 2012; Ward et al., 2018). BC deposition is the largest source of fresh snow albedo uncertainty (Flanner et al., 2007), and BC from Northern Hemisphere forest fires have the potential to increase snowmelt over portions of the GrIS (Ward et al., 2018). Furthermore, mineral dust concentrations can be several orders of magnitude higher than BC concentrations in Greenland and have a stronger overall impact on GrIS albedo (Carmagnola et al., 2013). There have also been many recent studies on the effect of biological activity on GrIS ablation zone albedo (e.g. Cook et al., 2017, 2020; Tedstone et al., 2017), but conditions do not appear to be suitable for sufficient biological darkening in the percolation zone (Cooper and Smith, 2019).

A portion of the observed GrIS summertime warming is driven by increased atmospheric blocking over Greenland (Hanna et al., 2013, 2016; Mernild et al., 2014) and changes in both the amount and optical thickness of GrIS cloud cover (Hofer et al., 2019; Van Tricht et al., 2016). The Greenland Blocking Index (GBI), which quantifies atmospheric blocking at the 500-hPa level directly over Greenland, has been increasing in all seasons since 1981, with a particularly rapid summertime (JJA) trend since 1991 of +1.87 a^{-1} (Hanna et al., 2016, 2018). Persistent blocking reduces precipitation in southeast coastal Greenland (Auger et al., 2017), reduces snowfall accumulation over the central and southern GrIS by displacing summertime storm tracks poleward (Lewis et al., 2019), reduces cloud cover (Delhasse et al., 2018; Hofer et al., 2017), and enhances warm air advection into western Greenland, further increasing melt

(Ballinger et al., 2017; van den Broeke et al., 2017). Several studies (Tedesco et al., 2013, 2016) suggest that increased temperatures are the main cause of GrIS melting; however, we explore here the hypothesis of Hofer et al. (2017) that enhanced GBI promotes surface melt, and thus reduced albedo, from a recent increase in summertime SWD due to diminished optically thick cloud cover. Delhasse et al. (2018) suggest that the 2000 – 2016 increase in persistent blocking events could amplify the SMB decrease by a factor of two if similar atmospheric conditions persist in the near future. If these anticyclonic circulation anomalies continue, we could see an additional 0.86 mm a^{-1} of sea level rise in a +2 °C warmer climate (Hofer et al., 2019).

Here, we examine the mechanisms controlling the recent decline in GrIS albedo by collecting concurrent measurements of albedo, OGS, and LAI concentrations during a 4400 km-long snowmobile traverse of the western GrIS percolation zone. In addition to assessing the relative importance of snow grain metamorphism and LAI on GrIS albedo decline, we examine the roles of summertime atmospheric Greenland blocking and increases in incoming shortwave radiation, caused by changes in optically thick GrIS cloud cover, on GrIS albedo.

2. Methods

2.1. Albedo and Optical Grain Size Measurements

We measured snow accumulation (Lewis et al., 2019), surface melt (Graeter et al., 2018), surface albedo, optical grain size, and snow impurities across the western GrIS percolation zone during the 2016 – 2017 Greenland Traverse for Accumulation and Climate Studies (GreenTrACS). In 2016 we traversed 860 km from Raven/Dye-2 northward to Summit Station, and in 2017 we made a 1230 km clockwise loop starting and ending at Summit Station (see Figure 1). Both traverses roughly followed the 2150 m elevation contour (Lewis et al., 2019).

Additionally, we measured snow albedo and optical grain size using a Malvern Panalytical (formerly Analytical Spectral Device; ASD) FieldSpec 4 spectroradiometer. The instrument measures spectrally resolved radiation from 350 to 1850 nm at resolutions between 3 nm in the visible/near-infrared and 10-12 nm in the infrared. We measured albedo 90 cm above the snow surface using a standard remote cosine receptor fore-optic (RCR) at the end of a 112.5 cm rod, using levelling bubbles to ensure instrument horizontality. We collected albedo values at 35

locations along the traverse route in April – June 2016, and at 29 locations in April – June 2017. Each albedo value represents an average of many individual measurements collected from 2 – 3 sites spaced several meters apart to account for albedo variability from fresh snow, sastrugi, and wind-compacted snow (Wang and Zender, 2010; Wright et al., 2014). At each site we collected five upward- and downward-looking pairs, each of which is an average of 60 individual instrument readings, to minimize the effects of passing clouds or blowing snow. Each measurement was made standing "down-sun" of the receptor to avoid blocking any direct radiation from the sensor.

After eliminating erroneous measurements ($> 3\sigma$), we made corrections for the solar zenith angle at measurement time, the angular response of the RCR, and the presence of the observer's body (following Carmagnola et al., 2013 and Wright et al., 2014). We then calculated the wavelength-integrated albedo (henceforth "broadband albedo", $\boldsymbol{\alpha_b}$) from the calculated spectral albedo $\boldsymbol{\alpha(\lambda)}$ and the measured incoming solar radiation $\boldsymbol{F\downarrow(\lambda)}$:

$$\boldsymbol{\alpha_b} = \frac{\int_{350}^{1850} \boldsymbol{\alpha(\lambda) F\downarrow(\lambda)\, d\lambda}}{\int_{350}^{1850} \boldsymbol{F\downarrow(\lambda)\, d\lambda}} \qquad (1)$$

We measured the near-surface snow OGS in snow pits at 13 firn core locations and at the end of six east-west spurs from the main traverse route, each approximately 40 – 50 km up- or down-slope from a firn core site (Figure 1). OGS was measured with a spectral method developed by Nolin and Dozier (2000), which uses the scaled band area of the 1030 nm absorption feature of snow (Figure 2b). The FieldSpec 4 contact probe emits a well-known source of light to measure reflectance that is used to calculate OGS, following methods from Adolph et al. (2017) and Nolin and Dozier (2000). We averaged OGS measurements collected every 5 cm in the upper 30 cm of the snow pit wall at each location, following the methods of Adolph et al. (2017) and Skiles and Painter (2017).

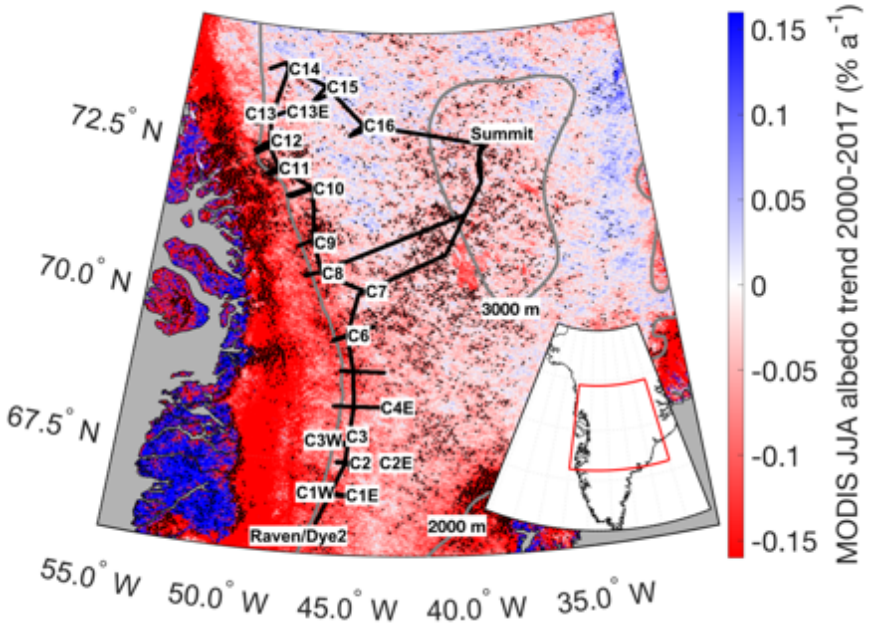

Figure 1. Trend in 2000-2017 June-August MODIS albedo (Hall et al., 2018) across the GrIS. Statistically significant grid cell trends are stippled black. The GreenTrACS route (black), and snow pit locations used in this study are also shown.

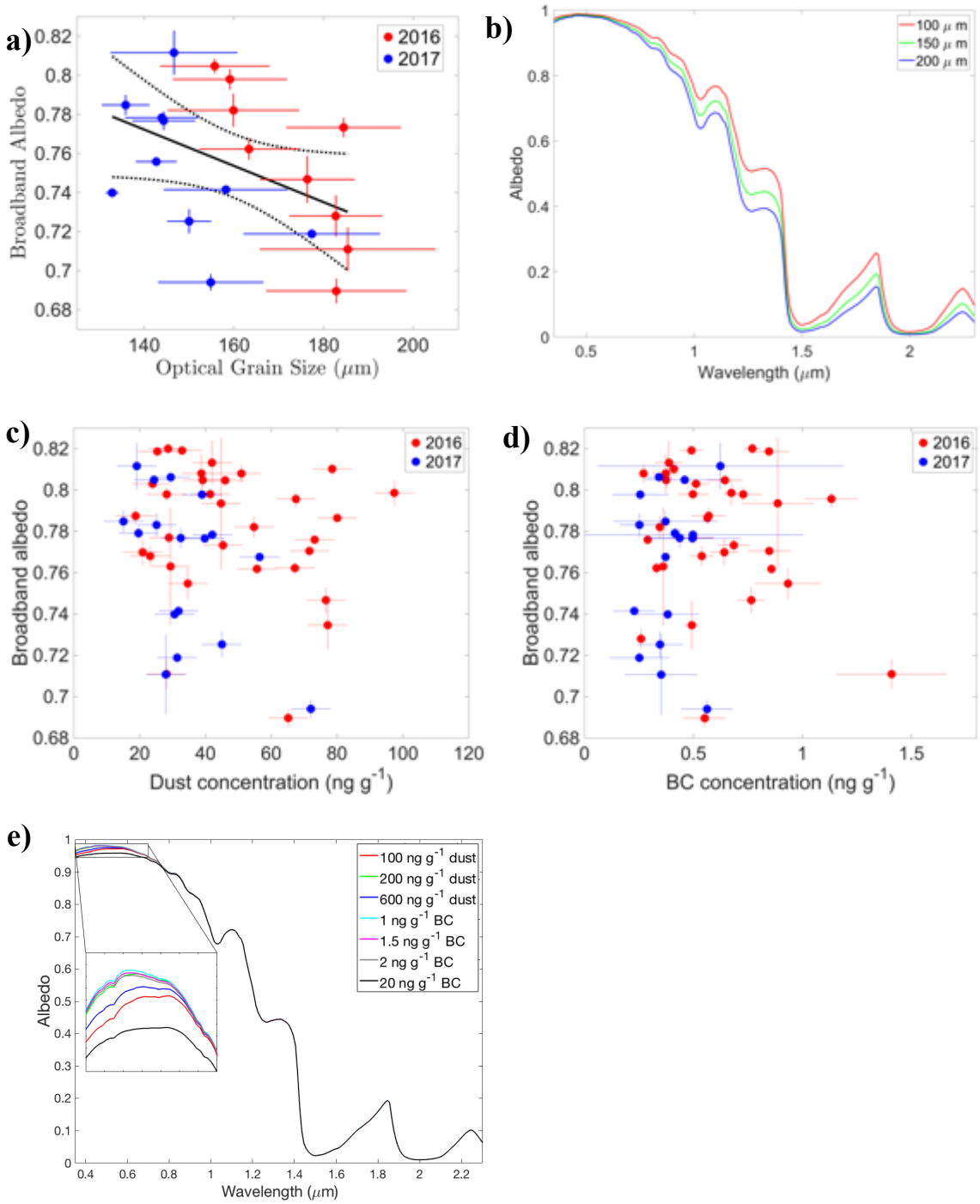

Figure 2. a) Relationship between broadband albedo and optical grain size for 2016 (red) and 2017 (blue) locations. Uncertainty bars represent one standard deviation. Note a statically significant negative correlation with p = 0.006 and R^2 = 0.349. b) SNICAR modeling results of clean snow with snow grain sizes of 100, 150, and 200 µm. These results show a significant decrease in albedo with larger grain sizes. Relationship between broadband albedo and c) dust and d) black carbon concentrations for 2016 (red) and 2017 (blue) locations. Note we do not observe statistically significant correlations for either relationship. e) SNICAR modeling results of snow with grain sizes of 150 µm and impurities of 100, 200, and 600 ppm dust and 1, 1.5, 2, and 20 ppb black carbon.

2.2. Snow Impurities

We collected snow impurity samples from 33 snow pits in 2016 and 18 snow pits in 2017 integrated over 0 – 1 cm, 1 – 15 cm, and 15 – 30 cm depths using pre-cleaned sample bottles. Samples were kept frozen during transport and prior to analysis. Samples were analyzed for mineral dust concentrations at the Dartmouth College Ice Core Laboratory using an Abakus (Klotz) laser particle detector (Simonsen et al., 2018), which continuously measures microparticle concentrations in 31 size bins from 1.0 – 15.0 μm diameter. We used a Single Particle Soot Photometer (SP2) in the Dibb Lab at the University of New Hampshire to analyze samples for BC concentration following the method of Lazarcik et al. (2017). The reported concentrations are the mean of at least three replicate measurements after being corrected by a deionized water blank sample. Impurity concentrations were averaged for all three collected depth ranges for each location. Uncertainties in BC and dust measurements are propagated from the standard deviation of replicate measurements and blank samples.

We use the Snow, Ice, and Aerosol Radiative (SNICAR) model (Flanner et al., 2007) to calculate spectral albedo for clean snow with various grain sizes, and for snow with BC and mineral dust concentrations similar to those observed in the field. SNICAR is a single-layer model that uses the two-stream radiative transfer solution of Toon et al. (1989) to calculate spectral albedo between 300 and 5000 nm. We used direct incident radiation, a solar zenith angle of 60° at Summit Greenland, snow grain radii of 100 – 200 μm, a snowpack thickness of 1000 m, snowpack density of 333 kg m^{-3}, uncoated BC concentrations of 1 – 20 ppb, dust concentrations of 100 – 600 ppm, and defaults for the remaining SNICAR parameters (Table S1).

3. Results and Discussion

3.1. Grain Size vs. Impurity Controls on Albedo

We find a statistically significant negative correlation between OGS (159.8 ± 17.2 μm; mean ± standard deviation) and broadband albedo along the traverse route, with a slope of -0.09 ± 0.05 % μm^{-1} ($p < 0.01$, $R^2 = 0.35$ Figure 2a). This relationship is consistent with previous studies, which observe that larger grain sizes have longer scattering paths and thus lower albedo (Flanner and Zender, 2006; Wiscombe and Warren, 1980)

In contrast to the significant OGS-albedo relationship, we find no relationship between dust concentrations and broadband albedo ($p = 0.24$; Figure 2c), nor between BC concentrations and broadband albedo ($p = 0.96$; Figure 2d). Similarly, we do not find significant relationships between dust and visible albedo ($p = 0.20$) or near infrared albedo ($p = 0.72$), nor between BC and visible albedo ($p = 0.88$) or near infrared albedo ($p = 0.14$). Likewise, a multivariate linear regression reveals no statistically significant relationship between the combined effect of dust and BC and broadband albedo ($p = 0.12$, $R^2 = 0.14$).

We find that grain size, rather than impurity concentration, is a primary control on albedo in the GrIS percolation zone. These results are supported by SNICAR experiments (see Table S1 and "SNICAR model results" section in the supplemental info), which indicate that BC and dust concentrations similar to those measured during the GreenTrACS campaign (or even an order of magnitude larger than measured) are not large enough to appreciably reduce broadband albedo (Figure 2e). However, grain sizes similar to those measured *in situ* can change the broadband albedo by 3 – 9% and can change spectral albedo across the visible and near-infrared wavelengths by 1.8 – 12.4% (Figure 2b). We emphasize that our results do not apply to the well documented 'dark snow zone' closer to the edges of the GrIS, where impurity concentrations are much larger than within the GreenTrACS region (Tedstone et al., 2017; Wientjes et al., 2011).

3.2. Albedo and Optical Grain Size Trends

We validate the regional climate model (RCM) Regional Atmospheric Climate Model (RACMO2.3p2; Noël et al., 2018) albedo and OGS output (see Figures S1 – S2) against our *in situ* measurements to examine albedo and OGS trends. We calculate June – August (JJA) albedo (Figure 3a) and snow grain size (Figure 3b) trends for each model grid cell over the 1996 – 2017 period. We choose this period to capture the recent positive phases of the Greenland Blocking Index (GBI) and to analyze the complete temporal coverage of AWS data. Our albedo results do not change when using Modèle Atmosphérique Régional (MARv4.5.2; 1948 – 2015; Fettweis et

al., 2016) output instead, however the grain size trends do not show similar spatial patterns (not shown).

Figure 3a-b shows that nearly the entire ice sheet has darkened and transitioned to larger surface snow grain sizes over the 1996 – 2017 period in RACMO2, with the exception of the NE region where grain sizes are slightly decreasing. For both RACMO2 and MAR we calculate statistically significant ($p < 0.05$) negative albedo trends of -0.02 to -0.04% a^{-1} and statistically significant positive snow grain size trends between 1 and 2.5 µm a^{-1} throughout the western GrIS.

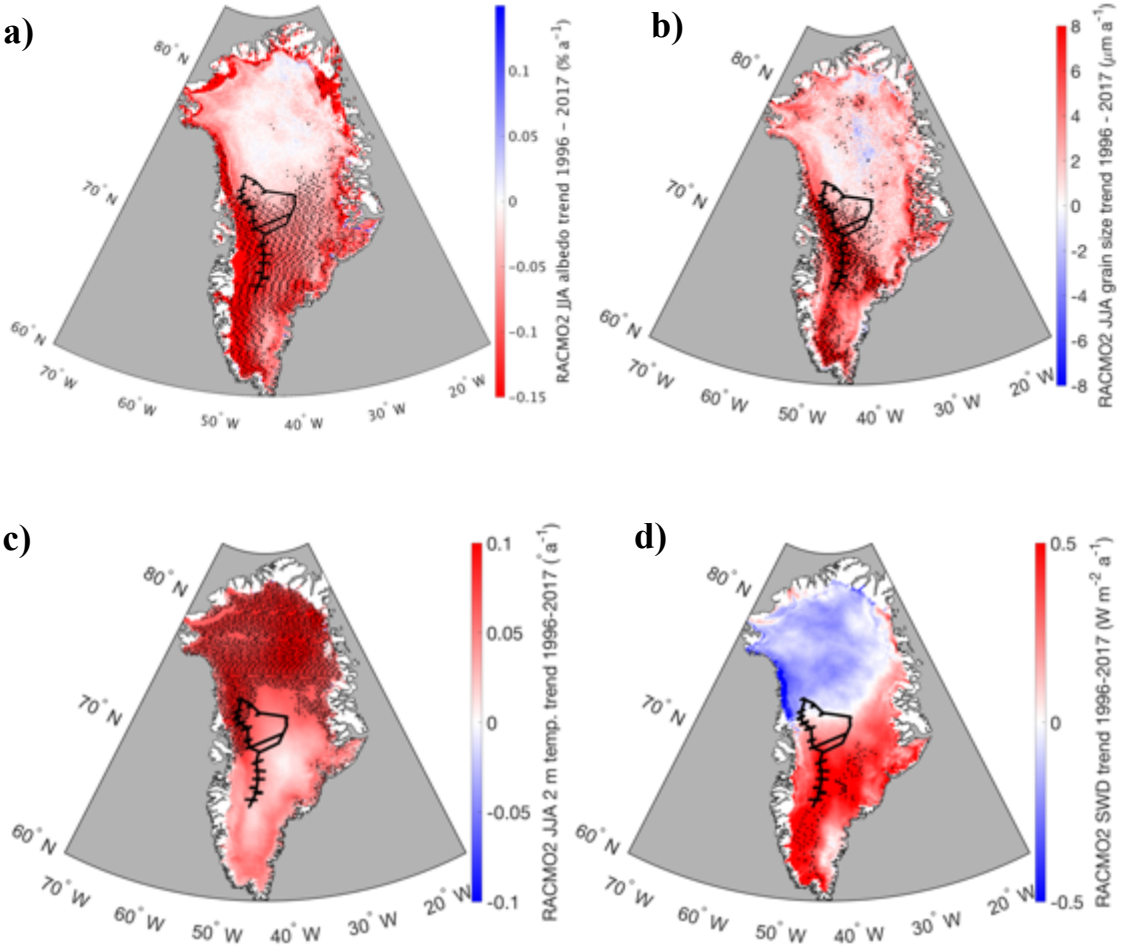

Figure 3. June - August a) albedo, b) optical grain size, c) temperature, and d) incoming shortwave radiation (SWD) trends for RACMO2 over 1996 – 2017. The GreenTrACS traverse is shown in black and statistically significant grid cell trends are stippled black.

It is possible that the Greenland-wide grain size increase is due in part to warmer GrIS surface temperatures. Average summer temperatures across interior Greenland increased 0.135 ± 0.047

°C a^{-1} from 2000 – 2013 (Hall et al., 2013; Reeves Eyre and Zeng, 2017). However, an analysis of both RACMO2 (Figure 3c) and MAR (Figure S3a) JJA temperature trends reveals warming across the entire GrIS with the largest warming (statistically significant) throughout the north in the region with the smallest trend in grain growth (Figure 3b). We hypothesize that snow grain growth and albedo decline across most of the GrIS, in addition to temperature increase, are driven by increased incoming shortwave radiation (SWD; Figure 3d and Figure S3b) and changes in summertime storm paths and frequency, both of which are related to stronger Greenland atmospheric blocking as discussed below.

3.3. The Role of Atmospheric Blocking in Albedo Decline

We find that stronger summertime Greenland blocking, defined as higher mean JJA GBI, is associated with lower GrIS summertime albedo. This is indicated by significant negative correlations between JJA GBI and JJA albedo across the GrIS in RACMO2 ($r = -0.55 \pm 0.04$, $p < 0.001$; Figure 4a) and MAR ($r = -0.36 \pm 0.06$, $p < 0.001$), with similarly strong negative correlations over the GreenTrACS region (RACMO2: $r = -0.43$, $p < 0.001$; MAR: $r = -0.65$, $p < 0.001$; Figure 4b).

We discuss two mechanisms by which stronger summertime blocking lowers GrIS albedo: (1) enhanced blocking reduces the number of storms that track over the southern half of the GrIS, causing a decrease in albedo due to longer intervals between accumulation events of high-albedo fresh snow (Figure S5a); (2) enhanced blocking causes a decrease in summertime optically thick cloud cover in the southern half of the GrIS (Figure 4d; Figure S5b; Hofer et al., 2017), which increases incoming shortwave radiation and enhances grain growth (and thereby lowers albedo) through snow metamorphism (van den Broeke et al., 2017; Moustafa et al., 2015).

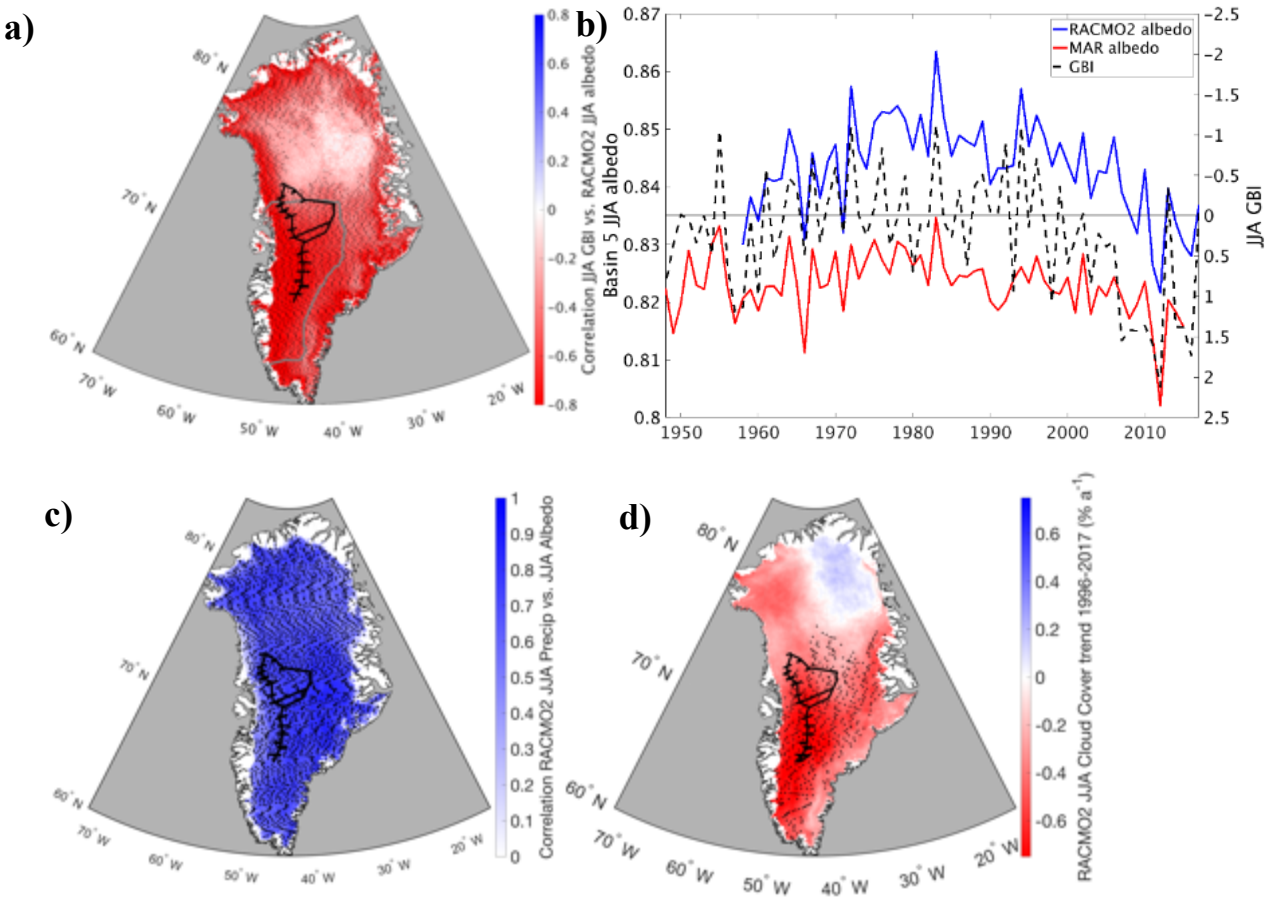

Figure 4. a) Correlation between June – August ERA-Interim JJA GBI and RACMO2 June – August broadband albedo over 1979 – 2017. Thin grey line indicates basin 5. b) 1948 – 2017 time series of JJA basin 5 broadband albedo for RACMO2 (blue) and MAR (red) along with June – August GBI (dashed black). c) Correlation between June – August RACMO2 precipitation and JJA albedo. d) June – August RACMO2 cloud cover trend for 1996 – 2015. The GreenTrACS traverse is shown in black and statistically significant trends are stippled black for all maps.

3.3.1 Reduction in Summertime Storms

Investigating the first mechanism, we find an average correlation of 0.65 ($p < 0.001$) between 1958 – 2017 JJA albedo and JJA precipitation in RACMO2 (Figure 4c) across the entire GrIS, indicating that summertime broadband albedo increases with fresh snow events when the surface replenishes with small (high-albedo) fresh snow grains. Lewis et al. (2019) found declining snowfall across the GreenTrACS region over 1996 – 2017 from both firn cores and geophysical measurements. Consistent with our hypothesis, we also find a correlation of 0.42 ($p < 0.001$) between the number of JJA storms and GrIS average JJA RACMO2 albedo. Here, storms are defined when sea level pressure at a 2.5º grid point is surrounded by grid points at least 1 hPa higher than the central point, following Serreze (2009) and Lewis et al. (2019). Dumont et al.

(2014) calculate that fewer than 20 cm of snow accumulation is sufficient to reset the albedo to the high values characteristic of fresh snow. Similarly, Flanner and Zender (2006) show a decrease in broadband albedo of 3 – 6% over a two-week period without snowfall.

We further evaluate the albedo increase from fresh snowfall using automatic weather station (AWS) data from the GC-Net archive (Steffen and Box, 2001). We examine 400 – 900 storm events (depending on AWS) that deposited at least 5 cm of fresh snow and contrast the average AWS albedo on the day before and the day after the storm. Our analysis from 1995 – 2019 reveals that after fresh snow deposition, albedo increases by 0.6 ± 0.2% ($n = 982$, $p < 0.001$) at GITS, 1.5 ± 0.2% ($n = 626$, $p < 0.001$) at Humboldt, 0.9 ± 0.2% ($n = 939$, $p < 0.001$) at Summit, 1.3 ± 0.2% ($n = 722$, $p < 0.001$) at TUNU-N, and 0.6 ± 0.3% ($n = 452$, $p < 0.001$) at NASA-E. These results confirm a significant albedo increase after fresh snowfall across an elevation range of 1860 to 3200 m a.s.l.

Having established significant relationships between GrIS JJA albedo and fresh snowfall, we now assess the role of Greenland blocking. We find a correlation of -0.48 ($p < 0.001$) between GrIS-wide RACMO2 JJA precipitation and JJA GBI (Figure S5a), and a correlation of -0.33 ($p < 0.05$) between the number of JJA storms and JJA GBI. These correlations indicate that stronger summertime blocking (higher GBI) reduces the number of storms crossing over Greenland and the amount of snowfall on the ice sheet (Lewis et al. 2019), thereby reducing albedo. The exception is NW Greenland, where stronger Greenland blocking causes higher precipitation (Figure S5a), suggesting that storm tracks were deflected poleward from southern and central Greenland (Lewis et al., 2019). Consistent with this hypothesis, we find a statistically significant decrease in the number of storms crossing the GreenTrACS region annually between 1958 – 1996 and 1996 – 2016 (14.61 ± 4.72 fewer storms; $p < 0.0001$). Most of this decrease occurred in spring (MAM; 3.28 ± 1.67; $p < 0.05$) and summer (JJA; 9.47 ± 2.71; $p < 0.0001$), as calculated with the methods from Lewis et al. (2019).

3.3.2 Increase in Shortwave Radiation

Summertime cloud cover over the GrIS has declined significantly since 1995 during the period of enhanced summer blocking (Hofer et al., 2017), with a trend of -0.51 ± 0.17% a^{-1} in

RACMO2 (1996 – 2013; Figure 4d) and -0.24 ± 0.05 % a^{-1} in MAR (1996 – 2015; Figure S3c). The cloud cover reduction is also confirmed by satellite observations, with a total decline of 14.1 ± 4.38% from 1994 – 2009 (Hofer et al., 2017). Likewise, Miller et al. (2015) calculate a decreased cloud radiative forcing at Summit Station. We calculate a correlation of -0.53 ($p < 0.001$) between MAR JJA cloud cover and JJA GBI (see Figure S5b), consistent with the hypothesis that stronger blocking (anticyclonic circulation) is largely responsible for the decreasing cloud cover trend (Hofer et al., 2017). The exception is NE Greenland, where RACMO2 cloud cover has increased from 1996 – 2015 (Figure 4d) and there is positive correlation with the GBI (Figure S5b). We hypothesize that the increase in incoming shortwave radiation in the southern half of the GrIS (Figure 3d) associated with the declining cloud cover has driven enlargement of surface snow grain sizes (Hofer et al., 2017), thereby lowering the summertime albedo and contributing to increased recent GrIS melting (e.g. Nghiem et al., 2012; Hofer et al., 2017; Graeter et al., 2018).

At Summit Station, the peak July shortwave cooling effect of clouds averages -18 W m^{-2}, with a 5th percentile approaching -55 W m^{-2}, while the annual average cloud radiative forcing is +33 W m^{-2} (Miller et al., 2015). However, Niwano et al. (2019) found that clouds reduced GrIS runoff by 0.8 – 1.6 Gt day^{-1} (totaling 70 – 157 Gt) during the 2012 – 2014 summers, and Hofer et al. (2017) estimate that summer melt is enhanced by 27 ± 13 Gt for every percent of JJA cloud cover reduction. Our findings suggest that one of the mechanisms by which reduced cloud cover leads to the enhanced GrIS surface melt documented in these studies is via larger grain sizes and the resulting albedo reduction.

During the 2012 melt event at Summit Station, surface snow metamorphism and phase change due to increased SWD and warmer temperatures (associated with the highest JJA GBI on record) induced a ~5% reduction in albedo and substantially contributed to melting (Keegan et al., 2014). Additionally, we find GC-Net AWS albedo reductions over the days following the 2012 melt event of 10.3 ± 1% ($p < 10^{-35}$) at GITS, 4.0 ± 0.96% ($p < 10^{-13}$) at Humboldt, 8.1 ± 1.3% ($p < 10^{-23}$) at TUNU-N, 3.6 ± 1.5% ($p < 10^{-6}$) at NASA-E, and 9.3 ± 1.3 ($p < 10^{-25}$) at NEEM. The albedo reductions during this widespread melt event during exceptionally strong Greenland blocking provide an extreme example of the effect of blocking on albedo via higher incoming

shortwave radiation and abnormally high surface temperature (Fausto et al., 2016). The 2012 widespread melt was enhanced by anomalously warm and moist air over Greenland, causing low-level liquid clouds to promote grain metamorphism (Bennartz et al., 2013).

We have shown that increased GBI may cause fewer storms over the southern half of the GrIS, which can reduce albedo through increased temperature and solar radiation due to fewer clouds and a decrease in the frequency of fresh snow. Grain size and albedo create a positive feedback via temperature, in which reduced albedo allows the snowpack to warm more quickly, further increasing the snow grain size, and contributing to additional albedo decline. Whether the recent increase in GBI will continue into the future is currently unclear, as none of the GBI outputs from the Coupled Model Intercomparison Project 5 (CMIP5) suite of global climate models accurately capture the recent summertime GBI increase (Hanna et al., 2018; Hofer et al., 2019). Thus, the importance of the GBI effect on albedo in future GrIS mass loss requires improved projections of future blocking.

4. Conclusions

We developed a new dataset of *in situ* albedo, impurity concentrations, and grain size measurements over the western percolation zone of the GrIS. We find statistically significant negative correlations between measured albedo and optical grain size, but no significant correlations between measured albedo and impurity concentrations. These correlations are consistent with SNICAR modeling, which indicates that observed impurity concentrations are not large enough to appreciably reduce broadband albedo, whereas observed grain sizes can lower the broadband albedo by at least 3%.

We hypothesize that stronger summertime Greenland blocking has significantly contributed to the decline in western GrIS percolation zone albedo by increasing snow grain sizes through two mechanisms: (1) a reduced number of storms that replenish GrIS albedo with fresh snow, and (2) reduced cloud cover and increased incoming shortwave radiation, promoting snow grain metamorphism and further reductions in albedo. Our results highlight the importance of improving GCM projections of future summertime Greenland blocking to accurately predict the

evolution of GrIS albedo and storm tracks, which ultimately influence precipitation and melt rates across the ice sheet.

5. Acknowledgements

This project was supported by the U.S. National Science Foundation (NSF) under grants ARC-1417678, ARC-1417921, and DGE-1313911. The FieldSpec4 was provided courtesy of Malvern Panalytical (formerly Analytical Spectral Device; ASD) as part of the Goetz Fellowship for both the 2016 and 2017 field seasons. We thank Xavier Fettweis and Brice Noel for providing the most recent MAR and RACMO2 regional climate model outputs. Our successful data collection would not have been possible without the support of CH2M Hill Polar Field Services, Kangerlussuaq International Science Support, the U.S. Ice Drilling Program, and the Air National Guard 109th Airlift Wing. Special thanks to Sean Birkel and the Danish Meteorological Institute for location-specific weather forecasts in Greenland, to Alden Adolph for assistance with albedo processing and data analysis, and to Eric Scheuer for assistance processing the black carbon snow samples.

All data used in this study is available through doi:10.18739/A2ZC7RV70.

6. Works Cited

Adolph, A. C., Albert, M. R., Lazarcik, J., Dibb, J. E., Amante, J. M. and Price, A.: Dominance of grain size impacts on seasonal snow albedo at open sites in New Hampshire, J. Geophys. Res., 122(1), 121–139, doi:10.1002/2016JD025362, 2017.

Alexander, P. M., Tedesco, M., Fettweis, X., Van De Wal, R. S. W., Smeets, C. J. P. P. and van den Broeke, M. R.: Assessing spatio-temporal variability and trends in modelled and measured Greenland Ice Sheet albedo (2000-2013), Cryosphere, 8(6), 2293–2312, doi:10.5194/tc-8-2293-2014, 2014.

Auger, J. D., Birkel, S. D., Maasch, K. A., Mayewski, P. A. and Schuenemann, K. C.: Examination of precipitation variability in southern Greenland, J. Geophys. Res., 122(12), 6202–6216, doi:10.1002/2016JD026377, 2017.

Ballinger, T. J., Hanna, E., Hall, R. J., Cropper, T. E., Miller, J., Ribergaard, M. H., Overland, J. E. and Høyer, J. L.: Anomalous blocking over Greenland preceded the 2013 extreme early melt

of local sea ice, Ann. Glaciol., 2013(March 2013), 1–10, doi:10.1017/aog.2017.30, 2017.
Bennartz, R., Shupe, M. D., Turner, D. D., Walden, V. P., Steffen, K., Cox, C. J., Kulie, M. S., Miller, N. B. and Pettersen, C.: July 2012 Greenland melt extent enhanced by low-level liquid clouds, Nature, 496(7443), 83–86, doi:10.1038/nature12002, 2013.
Box, J. E., Fettweis, X., Stroeve, J. C., Tedesco, M., Hall, D. K. and Steffen, K.: Greenland ice sheet albedo feedback: Thermodynamics and atmospheric drivers, Cryosphere, 6(4), 821–839, doi:10.5194/tc-6-821-2012, 2012.
van den Broeke, M. R., Bamber, J. L., Ettema, J., Rignot, E. J., Schrama, E., van de Berg, W. J., van Meijgaard, E., Velicogna, I. and Wouters, B.: Partitioning recent Greenland mass loss., Science, 326(5955), 984–6, doi:10.1126/science.1178176, 2009.
van den Broeke, M. R., Box, J. E., Fettweis, X., Hanna, E., Noël, B., Tedesco, M., van As, D., van de Berg, W. J. and van Kampenhout, L.: Greenland Ice Sheet Surface Mass Loss: Recent Developments in Observation and Modeling, Curr. Clim. Chang. Reports, 3(4), 345–356, doi:10.1007/s40641-017-0084-8, 2017.
Carmagnola, C. M., Domine, F., Dumont, M., Wright, P., Strellis, B., Bergin, M. H., Dibb, J. E., Picard, G., Libois, Q., Arnaud, L. and Morin, S.: Snow spectral albedo at Summit, Greenland: Measurements and numerical simulations based on physical and chemical properties of the snowpack, Cryosphere, 7(4), 1139–1160, doi:10.5194/tc-7-1139-2013, 2013.
Casey, K. A., Polashenski, C. M., Chen, J. and Tedesco, M.: Impact of MODIS sensor calibration updates on Greenland Ice Sheet surface reflectance and albedo trends, Cryosphere, 11(4), 1781–1795, doi:10.5194/tc-11-1781-2017, 2017.
Cook, J. M., Hodson, A. J., Taggart, A. J., Mernild, S. H. and Tranter, M.: A predictive model for the spectral “bioalbedo” of snow, J. Geophys. Res. Earth Surf., 122(1), 434–454, doi:10.1002/2016JF003932, 2017.
Cook, J. M., Tedstone, A. J., Williamson, C., McCutcheon, J., Hodson, A. J., Dayal, A., Skiles, M., Hofer, S., Bryant, R., McAree, O., McGonigle, A., Ryan, J., Anesio, A. M., Irvine-Fynn, T. D. L., Hubbard, A., Hanna, E., Flanner, M., Mayanna, S., Benning, L. G., Van As, D., Yallop, M., McQuaid, J. B., Gribbin, T. and Tranter, M.: Glacier algae accelerate melt rates on the south-western Greenland Ice Sheet, Cryosphere, 14(1), 309–330, doi:10.5194/tc-14-309-2020, 2020.
Cooper, M. G. and Smith, L. C.: Satellite remote sensing of the Greenland Ice Sheet Ablation Zone: A review, Remote Sens., 11(20), 10–13, doi:10.3390/rs11202405, 2019.

Delhasse, A., Fettweis, X., Kittel, C., Amory, C. and Agosta, C.: Brief communication: Impact of the recent atmospheric circulation change in summer on the future surface mass balance of the Greenland Ice Sheet, Cryosphere, 12(11), 3409–3418, doi:10.5194/tc-12-3409-2018, 2018.
Dumont, M., Brun, E., Picard, G., Michou, M., Libois, Q., Petit, J., Geyer, M., Morin, S. and Josse, B.: Contribution of light-absorbing impurities in snow to Greenland's darkening since 2009, Nat. Geosci., 7(7), 509–512, doi:10.1038/ngeo2180, 2014.
Fausto, R. S., As, D., Box, J. E., Colgan, W., Langen, P. L. and Mottram, R. H.: The implication of nonradiative energy fluxes dominating Greenland ice sheet exceptional ablation area surface melt in 2012, Geophys. Res. Lett., 43(6), 2649–2658, doi:10.1002/2016GL067720, 2016.
Fettweis, X., Box, J. E., Agosta, C., Amory, C., Kittel, C. and Gallée, H.: Reconstructions of the 1900-2015 Greenland ice sheet surface mass balance using the regional climate MAR model, Cryosph. Discuss., (November), 1–32, doi:10.5194/tc-2016-268, 2016.
Flanner, M. G. and Zender, C. S.: Linking snowpack microphysics and albedo evolution, J. Geophys. Res. Atmos., 111(12), 1–12, doi:10.1029/2005JD006834, 2006.
Flanner, M. G., Zender, C. S., Randerson, J. T. and Rasch, P. J.: Present-day climate forcing and response from black carbon in snow, J. Geophys. Res. Atmos., 112(11), 1–17, doi:10.1029/2006JD008003, 2007.
Flanner, M. G., Liu, X., Zhou, C., Penner, J. E. and Jiao, C.: Enhanced solar energy absorption by internally-mixed black carbon in snow grains, Atmos. Chem. Phys., 12(10), 4699–4721, doi:10.5194/acp-12-4699-2012, 2012.
Graeter, K., Osterberg, E. C., Ferris, D., Hawley, R. L., Marshall, H. P. and Lewis, G.: Ice Core Records of West Greenland Surface Melt and Climate Forcing, Geophys. Res. Lett., doi:10.1002/2017GL076641, 2018.
Hall, D. K., Comiso, J. C., DiGirolamo, N. E., Shuman, C. A., Box, J. E. and Koenig, L. S.: Variability in the surface temperature and melt extent of the Greenland ice sheet from MODIS, Geophys. Res. Lett., 40(10), 2114–2120, doi:10.1002/grl.50240, 2013.
Hall, D. K., Cullather, R. I., DiGirolamo, N. E., Comiso, J. C., Medley, B. C. and Nowicki, S. M.: A multilayer surface temperature, surface albedo, and water vapor product of Greenland from MODIS, Remote Sens., 10(4), 1–17, doi:10.3390/rs10040555, 2018.
Hanna, E., Jones, J. M., Cappelen, J., Mernild, S. H., Wood, L., Steffen, K. and Huybrechts, P.: The influence of North Atlantic atmospheric and oceanic forcing effects on 1900-2010

Greenland summer climate and ice melt/runoff, Int. J. Climatol., 33(4), 862–880, doi:10.1002/joc.3475, 2013.
Hanna, E., Cropper, T. E., Hall, R. J. and Cappelen, J.: Greenland Blocking Index 1851-2015: a regional climate change signal, Int. J. Climatol., 36(15), 4847–4861, doi:10.1002/joc.4673, 2016.
Hanna, E., Fettweis, X. and Hall, R. J.: Recent changes in summer Greenland blocking captured by none of the CMIP5 models, Cryosph. Discuss., 1–8, doi:10.5194/tc-2018-91, 2018.
Hofer, S., Bamber, J., Tedstone, A. J. and Fettweis, X.: Decreasing clouds drives the recent mass loss on the Greenland Ice Sheet, Sci. Adv., 3, 2017.
Hofer, S., Tedstone, A. J., Fettweis, X. and Bamber, J. L.: Cloud microphysics and circulation anomalies control differences in future Greenland melt, Nat. Clim. Chang., 9(7), 523–528, doi:10.1038/s41558-019-0507-8, 2019.
De La Peña, S., Howat, I. M., Nienow, P. W., van den Broeke, M. R., Mosley-Thompson, E., Price, S. F., Mair, D., Noël, B. and Sole, A. J.: Changes in the firn structure of the western Greenland Ice Sheet caused by recent warming, Cryosphere, 9(3), 1203–1211, doi:10.5194/tc-9-1203-2015, 2015.
Lazarcik, J., Dibb, J. E., Adolph, A. C., Amante, J. M., Wake, C. P., Scheuer, E., Mineau, M. M. and Albert, M. R.: Major fraction of black carbon is flushed from the melting New Hampshire snowpack nearly as quickly as soluble impurities, J. Geophys. Res. Atmos., 122(1), 537–553, doi:10.1002/2016JD025351, 2017.
Lewis, G., Osterberg, E., Hawley, R., Marshall, H. P., Meehan, T., Graeter, K., McCarthy, F., Overly, T., Thundercloud, Z. and Ferris, D.: Recent precipitation decrease across the western Greenland ice sheet percolation zone, Cryosph., 13(11), 2797–2815, doi:10.5194/tc-13-2797-2019, 2019.
McGrath, D., Colgan, W., Bayou, N., Muto, A. and Steffen, K.: Recent warming at Summit, Greenland: Global context and implications, Geophys. Res. Lett., 40(10), 2091–2096, doi:10.1002/grl.50456, 2013.
Mernild, S. H., Hanna, E., Mcconnell, J. R., Sigl, M., Beckerman, A. P., Yde, J. C., Cappelen, J., Malmros, J. K. and Steffen, K.: Greenland precipitation trends in a long-term instrumental climate context (1890-2012): Evaluation of coastal and ice core records, Int. J. Climatol., 35(2), 303–320, doi:10.1002/joc.3986, 2014.
Miller, N. B., Shupe, M. D., Cox, C. J., Walden, V. P., Turner, D. D. and Steffen, K.: Cloud

radiative forcing at Summit, Greenland, J. Clim., 28(15), 6267–6280, doi:10.1175/JCLI-D-15-0076.1, 2015.
Moustafa, S. E., Rennermalm, A. K., Smith, L. C., Miller, M. A., Mioduszewski, J. R., Koenig, L. S., Hom, M. G. and Shuman, C. A.: Multi-modal albedo distributions in the ablation area of the southwestern Greenland Ice Sheet, Cryosphere, 9(3), 905–923, doi:10.5194/tc-9-905-2015, 2015.
Nghiem, S. V., Hall, D. K., Mote, T. L., Tedesco, M., Albert, M. R., Keegan, K. M., Shuman, C. A., DiGirolamo, N. E. and Neumann, G.: The extreme melt across the Greenland ice sheet in 2012, Geophys. Res. Lett., 39(20), 6–11, doi:10.1029/2012GL053611, 2012.
Niwano, M., Hashimoto, A. and Aoki, T.: Cloud-driven modulations of Greenland ice sheet surface melt, Sci. Rep., 9(1), 1–8, doi:10.1038/s41598-019-46152-5, 2019.
Noël, B., van de Berg, W. J., Van Wessem, J. M., Van Meijgaard, E., Van As, Di., Lenaerts, J. T. M., Lhermitte, S., Munneke, P. K., Smeets, C. J. P. P., Van Ulft, L. H., Van De Wal, R. S. W. and Van Den Broeke, M. R.: Modelling the climate and surface mass balance of polar ice sheets using RACMO2 - Part 1: Greenland (1958-2016), Cryosphere, 12(3), 811–831, doi:10.5194/tc-12-811-2018, 2018.
Nolin, A. W. and Dozier, J.: A hyperspectral method for remotely sensing the grain size of snow, Remote Sens. Environ., 74(2), 207–216, doi:10.1016/S0034-4257(00)00111-5, 2000.
Polashenski, C. M., Dibb, J. E., Flanner, M. G., Chen, J. Y., Courville, Z. R., Lai, A. M., Schauer, J. J., Shafer, M. M. and Bergin, M. H.: Neither dust nor black carbon causing apparent albedo decline in Greenland's dry snow zone: Implications for MODIS C5 surface reflectance, Geophys. Res. Lett., 42(21), 9319–9327, doi:10.1002/2015GL065912, 2015.
Reeves Eyre, J. E. J. and Zeng, X.: Evaluation of Greenland near surface air temperature datasets, Cryosphere, 11(4), 1591–1605, doi:10.5194/tc-11-1591-2017, 2017.
Serreze, M.: Northern Hemisphere cyclone locations and characteristics from NCEP/NCAR reanalysis data, Verison 1, Natl. Snow Ice Data Center, Boulder, CO, Digit. media.[Available online http//nsidc. org/data/nsidc-0423. html.], 2009.
Simonsen, M. F., Cremonesi, L., Baccolo, G., Bosch, S., Delmonte, B., Erhardt, T., Astrid Kjær, H., Potenza, M., Svensson, A. and Vallelonga, P.: Particle shape accounts for instrumental discrepancy in ice core dust size distributions, Clim. Past, 14(5), 601–608, doi:10.5194/cp-14-601-2018, 2018.

Skiles, S. M. and Painter, T. H.: Daily evolution in dust and black carbon content, snow grain size, and snow albedo during snowmelt, Rocky Mountains, Colorado, J. Glaciol., 63(237), 118–132, doi:10.1017/jog.2016.125, 2017.

Steffen, K. and Box, J. E.: Surface climatology of the Greenland ice sheet : Overview of study area . Monthly mean sea level pressure fields for (b) January , November the National Centers for Environmental Prediction, J. Geophys. Res., 106(33), 951–964, doi:10.1029/2001JD900161, 2001.

Tedesco, M., Fettweis, X., Mote, T., Wahr, J., Alexander, P., Box, J. E. and Wouters, B.: Evidence and analysis of 2012 Greenland records from spaceborne observations, a regional climate model and reanalysis data, Cryosph., 7(2), 615–630, doi:10.5194/tc-7-615-2013, 2013.

Tedesco, M., Doherty, S., Fettweis, X., Alexander, P. M., Jeyaratnam, J. and Stroeve, J. C.: The darkening of the Greenland ice sheet: Trends, drivers, and projections (1981-2100), Cryosphere, 10(2), 477–496, doi:10.5194/tc-10-477-2016, 2016.

Tedstone, A. J., Bamber, J. L., Cook, J. M., Williamson, C. J., Fettweis, X., Hodson, A. J. and Tranter, M.: Dark ice dynamics of the south-west Greenland Ice Sheet, Cryosphere, 11(6), 2491–2506, doi:10.5194/tc-11-2491-2017, 2017.

Toon, O. B., McKay, C. P., Ackerman, T. P. and Santhanam, K.: Rapid calculation of radiative heating rates and photodissociation rates in inhomogeneous multiple scattering atmospheres, J. Geophys. Res., 94(D13), 287–301, 1989.

Van Tricht, K., Lhermitte, S., Lenaerts, J. T. M., Gorodetskaya, I. V., L'Ecuyer, T. S., Noël, B., van den Broeke, M. R., Turner, D. D. and Van Lipzig, N. P. M.: Clouds enhance Greenland ice sheet meltwater runoff, Nat. Commun., 7(May 2015), doi:10.1038/ncomms10266, 2016.

Wang, X. and Zender, C. S.: MODIS snow albedo bias at high solar zenith angles relative to theory and to in situ observations in Greenland, Remote Sens. Environ., 114(3), 563–575, doi:10.1016/j.rse.2009.10.014, 2010.

Ward, J. L., Flanner, M. G., Bergin, M., Dibb, J. E., Polashenski, C. M., Soja, A. J. and Thomas, J. L.: Modeled Response of Greenland Snowmelt to the Presence of Biomass Burning-Based Absorbing Aerosols in the Atmosphere and Snow, J. Geophys. Res. Atmos., 123(11), 6122–6141, doi:10.1029/2017JD027878, 2018.

Warren, S. G. and Wiscombe, W. J.: A Model for the Spectral Albedo of Snow. II: Snow Containing Atmospheric Aerosols, J. Atmos. Sci. [online] Available from:

http://journals.ametsoc.org.lsc-proxy.libraries.vsc.edu/doi/pdf/10.1175/1520-0469(1980)037%3C2734:AMFTSA%3E2.0.CO;2, 1980.

Wientjes, I. G. M., Van De Wal, R. S. W., Reichart, G. J., Sluijs, A. and Oerlemans, J.: Dust from the dark region in the western ablation zone of the Greenland ice sheet, Cryosphere, 5(3), 589–601, doi:10.5194/tc-5-589-2011, 2011.

Wiscombe, W. J. and Warren, S. G.: A model for the spectral albedo of snow. I: Pure snow, J. Atmos. Sci., 37(12), 2712–2733, doi:10.1175/1520-0469(1980)037<2734:AMFTSA>2.0.CO;2, 1980.

Wright, P., Bergin, M., Dibb, J. E., Lefer, B., Domine, F., Carman, T., Carmagnola, C., Dumont, M., Courville, Z., Schaaf, C. and Wang, Z.: Comparing MODIS daily snow albedo to spectral albedo field measurements in Central Greenland, Remote Sens. Environ., 140, 118–129, doi:10.1016/j.rse.2013.08.044, 2014.

Zwally, H. J., Giovinetto, M. B., Li, J., Cornejo, H. and Beckley, M.: Mass changes of the Greenland and Antarctica ice sheets and shelves and contributions to sea level rise: 1992-2002, J. Glaciol., 51(175), 509, doi:10.3189/172756505781829007, 2005.

Zwally, H. J., Li, J., Brenner, A. C., Beckley, M., Cornejo, H. G., Dimarzio, J., Giovinetto, M. B., Neumann, T. a, Robbins, J., Saba, J. L., Yi, D. and Wang, W.: Greenland ice sheet mass balance : distribution of increased mass loss with climate warming ; 2003–07 versus 1992–2002, J. Glaciol., 57(201), 88–102, doi:10.3189/002214311795306682, 2011.